

# Electrostatic Precipitation in nearly pure Gaseous Nitrogen

Charles Buhler (1), Carlos Calle (2), Sid Clements (3), Bobby Cox (1) and Mindy Ritz (1)

(1) Electrostatics and Surface Physics Laboratory, ASRC Aerospace, Kennedy Space Center, FL 32899, USA  
tel.: 321-867-4861, fax: 321-867-7965, e-mail: [Charles.R.Buhler@nasa.gov](mailto:Charles.R.Buhler@nasa.gov)

(2) Electrostatics and Surface Physics Laboratory, NASA, Kennedy Space Center, FL 32899, USA  
tel.: 321-867-3274, fax: 321-867-4489, e-mail: [carlos.i.calle@nasa.gov](mailto:carlos.i.calle@nasa.gov)

(3) Department of Physics and Astronomy, Appalachian State University, Boone, NC 28608, USA  
tel.: 868-262-2447, fax: 828-262-2049, email: [clementsjs@appstate.edu](mailto:clementsjs@appstate.edu)

**Abstract** – Electrostatic precipitation was performed in a nearly pure gaseous nitrogen system as a possible remedy for black dust contaminant from high pressure 6000 psi lines at the NASA Kennedy Space Center. The results of a prototype electrostatic precipitator that was built and tested using nitrogen gas at standard atmospheric pressures is presented. High voltage pulsed waveforms are generated using a rotating spark gap system at 30 Hz. A unique dust delivery system utilizing the Venturi effect was devised that supplies a given amount of dust per unit time for testing purposes.

**Key words:** Dust contamination, electrostatic precipitation, rotating spark gap, nitrogen gas, high voltage.

## 1.0 Background

The Electrostatics and Surface Physics Laboratory at NASA Kennedy Space Center (KSC) was tasked to remove black dust contamination from KSC and the Cape Canaveral Air Force Station (CCAFS) gaseous nitrogen (GN<sub>2</sub>) lines using Electrostatic Precipitation (EP). Although the gas delivered to NASA KSC and CCAFS is well within specifications, conventional particulate filtration techniques have not eliminated the problem of tiny particles passing through 5-10 micron filter elements and re-entrainment of particulates along the over 40 miles of GN<sub>2</sub> pipeline throughout KSC and the CCAFS has been a continuing and unresolved problem. The gas is supplied by Air Liquide America Corporation (ALAC) which creates GN<sub>2</sub> from an air separation process to support day-to-day operations and supplements this with liquid nitrogen (LN<sub>2</sub>) vaporization during high-flows such as Shuttle launch count down. There is a six inch main supply line that operates between 5400 psig and 6800 psig depending on range support requirements and there are over 34 miles of underground GN<sub>2</sub> pipeline on KSC and CCAFS. Typical operations can require a system output as high as 24,000 SCFM.

Black dust has been found to be present in the lines even though extensive cleaning procedures such as blow-down and filtration methods have been implemented to reduce or eliminate the black dust. The dust most likely originates from the continual degradation of the piston rings at ALAC and contains PTFE as well as several metal oxides. An excellent reference providing background to the black dust problem is provided by Gibson *et al.*, 2005 [1].

One possible method to remove black dust contamination is electrostatic precipitation. Electrostatic precipitation has been used extensively for over 100 years to remove particulate contamination. Although precipitation is used commonly used throughout several industries, the technology for removal of particulates in certain gases other than air is limited. Furthermore, electrostatic precipitation performed at static pressures of 150 psi or above is rarely encountered. It was the aim of this study to see if electrostatic precipitation was feasible.

In order to test the feasibility of electrostatic precipitation, certain properties of the dust must be known such as the volume resistivity and the particle size distribution (PSD). Volume resistivity plays a key role in determining whether the dust is susceptible to back-ionization while the PSD of the black dust determines the efficiencies possible using electrostatic precipitation.

## 1.1 Volume resistivity

Measurements of the volume resistivity of the material not only gives an indication of the likelihood for the particles to acquire charge via corona, a necessity for particle collection, but it will also measure their ability to dissipate charge. As a charged dust accumulates on the collection plate, the electric field increases with each additional layer until electrical breakdown is reached. The breakdown causes a mini explosion of the dust layer resulting in re-entrainment of particles back into the gas flow. This phenomenon is called back-ionization and is a primary constraint for the design and use of precipitators. Charge must be allowed to flow through the dust to the collection and not remain on the outer surface for this to be avoided. This phenomenon usually prevents electrostatic precipitation of highly resistive dusts.

Materials with high volume resistivities such as *insulators* typically have resistivities higher than  $10^9 \Omega\cdot\text{m}$  and usually acquire larger amounts of charge during triboelectrification. They also sustain that charge longer than *statically dissipative* materials with resistivities between  $10^6$  and  $10^9 \Omega\cdot\text{m}$  and *conductive* materials with resistivities below  $10^6 \Omega\cdot\text{m}$ . Measurements typically involve placing the sample between two electrodes, applying a known voltage  $V$  and monitoring the resulting current  $I$ . The volume resistivity is

$$R_v = \frac{V}{I} \frac{A}{d}$$

where  $A$  is the electrode area and  $d$  is the sample thickness. Volume resistivity values are only successful if there is a steady current for the applied voltage which ranges vary from 100 volts up to 10 kV depending upon the expected resistivity values. In order for back-ionization not to occur requires the powder to have resistivities less than  $10^{10}$ - $10^{11} \Omega\cdot\text{m}$ .

Several tests were performed on the black dust under extremely dry conditions with relative humidities less than 1% using a dielectric test cell built to comply with ASTM D-150 [2]. The values for the volume resistivity measured between  $9.4 \times 10^5 \Omega\cdot\text{m}$  and  $1.18 \times 10^6 \Omega\cdot\text{m}$  meaning

that the black dust is *statically dissipative*. Therefore, the black dust should not be subject to back-ionization and re-entrainment may not be a problem.

The measured range of the volume resistivity shows that the black dust is ideal for electrostatic precipitation. The PTFE components of the black dust particles in the dust allow some electrical resistivity necessary for charge to collect on them while the metallic components are responsible for the charge to dissipate through a deposited dust layer. Thus the precipitation of black dust particles should be possible provided the ions are available in the gas.

## 1.2 Particle Size Distribution

Several tests were performed using a TSI Model 3321 Aerodynamic Particle Sizer which records the aerodynamic diameter of an aerosolized particle. The Model 3321 is specifically engineered to perform aerodynamic size measurements in real time using low particle accelerations. Time-of-flight particle sizing technology involves measuring the acceleration of aerosol particles in response to the accelerated flow of the sample aerosol through a nozzle. The aerodynamic size of a particle determines its rate of acceleration, with larger particles accelerating more slowly due to increased inertia. As particles exit the nozzle, the time of flight between the Model 3321's two laser beams is recorded and converted to aerodynamic diameter using a calibration curve. Before black dust particles entered into the Model 3321 they first were aerosolized using TSI Model 3343 Small Scale Powder Dispenser. The final configuration is one in which the Model 3321 sits atop the Model 3343 to ensure that the aerosol is measured immediately after it is created.

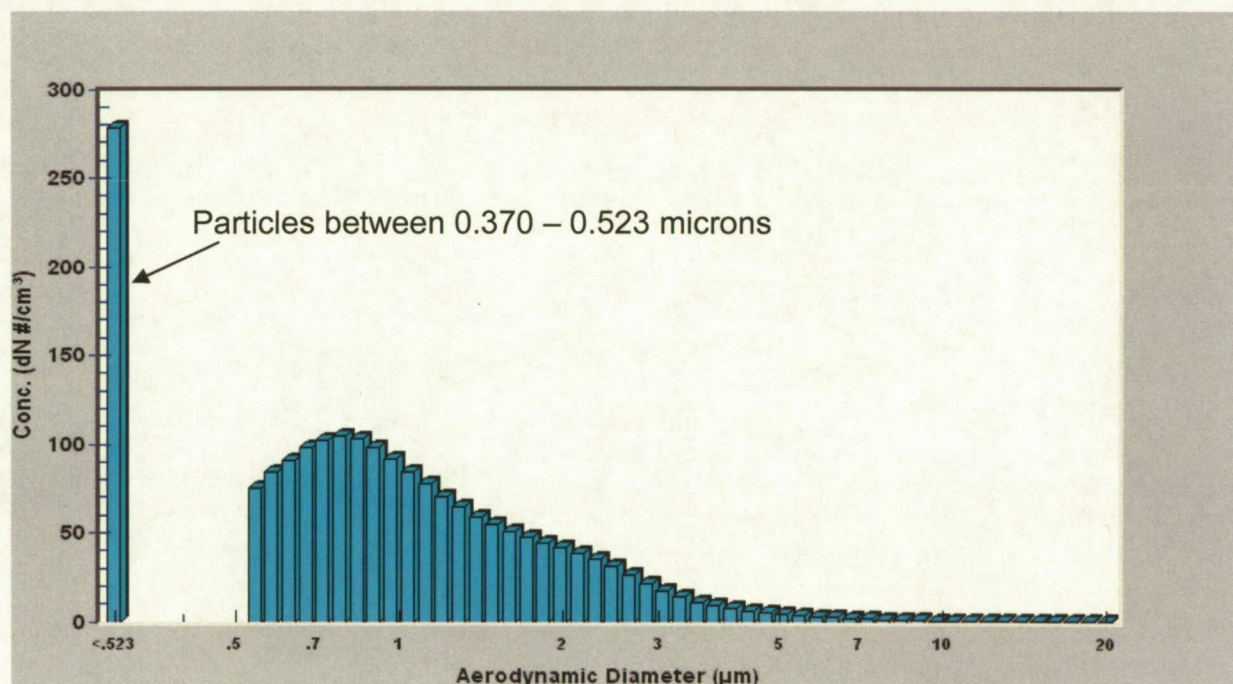


Figure 1. Measurements of the PSD of black dust using the TSI Model 3321 Aerodynamic Particle Sizer.

An example of the PSD for the black dust as measured by the 3321 Aerodynamic Particle Sizer is given in Figure 1. For particles between the sizes of 0.370 and 0.523 microns, only the



scattered light is captured by the detectors of the instrument and the resolution cannot be determined. However, the particles within this range can still be counted accurately. For the 7,682,980 particles measured during this black dust test, 6,679,050 fell within this size range. The distribution above 0.5 microns is described as having a mean of 1.33  $\mu\text{m}$ , a median of 1.00  $\mu\text{m}$  and a mode of 0.777  $\mu\text{m}$ . Several independent tests confirmed that black dust particles are comprised of particles  $\sim 0.8 \mu\text{m}$  in diameter.

The PSD is accurately fit using a log-normal size distribution as opposed to a Gaussian or normal distribution according to Figure 2. The log-normal distribution appears commonly for PSD of many processes which confirms the work of the famous Russian mathematician who showed that the log-normal distribution occurs in any process which produces fine particles from bulk materials [3]. Therefore this distribution is typical for fine particles, and other distributions must be regarded as peculiar.

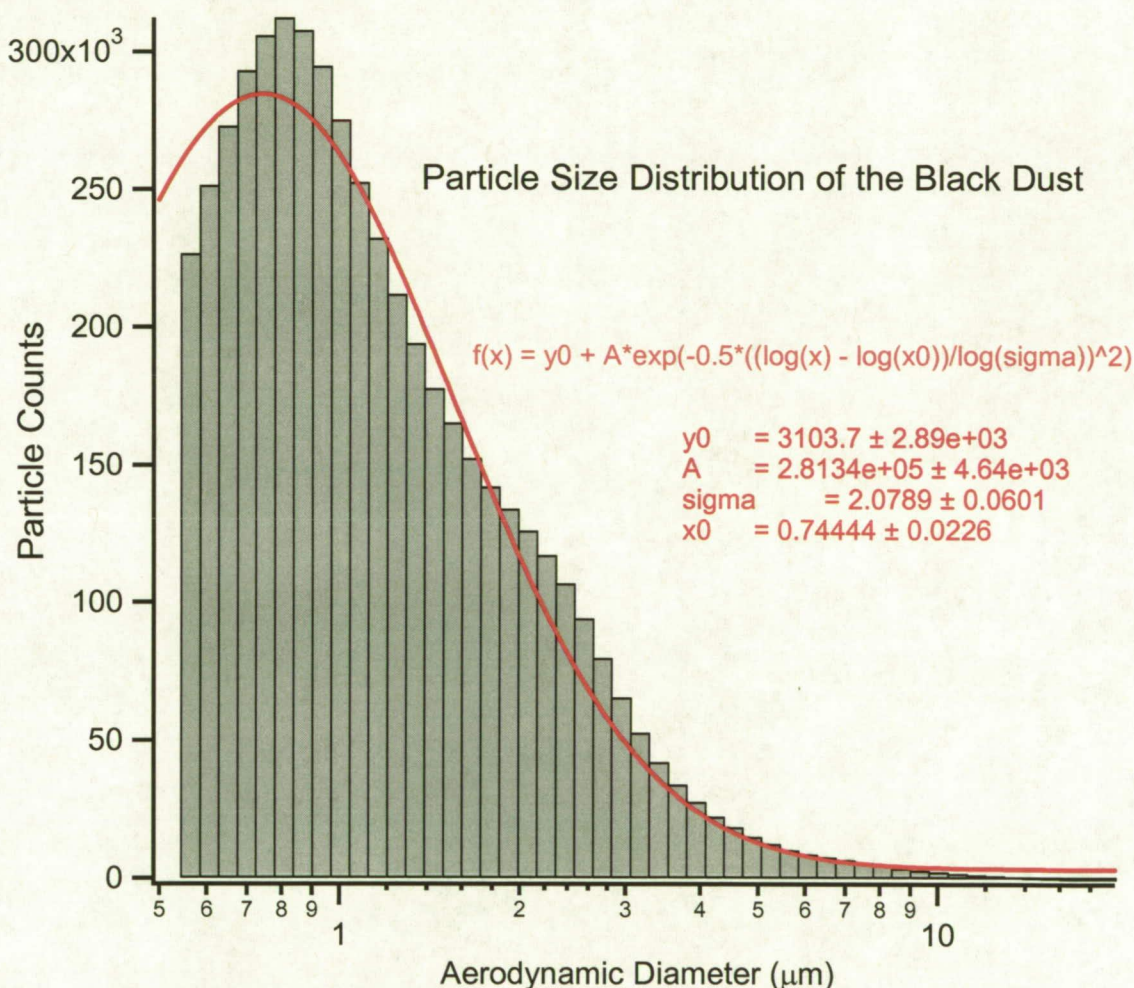


**Figure 2.** The log-normal distribution of the black dust along with the fitting parameters used to generate the fit (red line).



The geometric mean of the distribution is 0.7444 microns and the geometric standard deviation is 2.0789 microns. Knowledge of the PSD can be used to estimate the efficiency of an electrostatic precipitator provided a geometry is chosen.

## 2.0 Efficiency Estimates

The simplest geometry for an electrostatic precipitator is that of the wire-cylinder geometry. Application of high voltage to the center wire creates corona ions that attach and subsequently charge the incoming dust particles that now must follow electric field lines and drift toward the sides of the cylinder to be collected.

Once the geometry for precipitation is chosen, its dimensions must be calculated based on several parameters including gas flow rates, collection areas and particle migration velocities that gives the highest efficiency. The simplest theory that describes the efficiency  $Q$  as a function of those design parameters is given by the Deutsch equation

$$Q = 1 - e^{-(A/\dot{V})w}$$

where  $A$  is the collection area,  $\dot{V}$  is the flow rate and  $w$  is the particle migration velocity [4]. The migration velocity is a measure of how fast the charge particles move toward the collector and is usually on the order of 10 cm/sec [5].

Electrostatic precipitation requires that the gas velocity be below 2 m/s to prevent re-entrainment. The current GN<sub>2</sub> system is held at pressures in excess of 6000 psi. In order to accommodate pressures of this magnitude, the piping required is usually of small diameter ~5.1 inches ID thick-walled pipe. Minimizing the radius of the precipitator is advantageous since it decreases the drift time for the charged particles. However, the radius can not be made too small since the gas velocity will increase above 2 m/s. Therefore a radius of 1 inch was chosen as a minimum radius to show that electrostatic precipitation can work at even the maximum gas flow velocity.

To estimate the gas velocity we first divide the pipe pressure 6800 psi (max) by standard atmospheric pressure 14.7 psi which gives a factor of 462.5. Therefore, using the maximum flow rate of 24,000 SCFM for the lines is equivalent to 51.89 actual cubic feet per minute (CFM) which is 1469.5 liters per minute (lpm) or 0.02449 m<sup>3</sup>/sec. The gas flow velocity for a 5.1 inch diameter pipe is 1.8 m/sec which is matched by our electrostatic precipitator by using a flow rate of 7.94 CFM or 225 lpm.

Using these parameters, the Deutsch equation above predicts an efficiency of 96.8% for a 32 inch long precipitator which is quite good considering that in practice the precipitator would rarely be expected to operate at the maximum flow rate at the maximum pressure. Lowering either of these parameters would significantly increase the efficiency. For example a flow rate of 150 lpm would be 99.4% efficient while a flow rate of 100 lpm would be 99.95% efficient. Flow rates can be decreased by increasing the radius of the precipitator. Other methods of improving efficiency include adding an additional foot of collection area to the precipitator which gives 99.1%. In practice it is not uncommon for electrostatic precipitators to have efficiencies greater than 99%.



The efficiencies mentioned above use the standard migration velocity of 10 cm/sec however one can also estimate the drift velocity using [5]

$$w = \frac{\epsilon_0 a E_C E_p}{\eta}$$

as the form of the migration velocity where  $\epsilon_0$  is  $8.85 \times 10^{-12}$  F/m the permittivity of free space,  $\eta$  is the gas viscosity,  $a$  is the radius of the particle,  $E_C$  is the DC corona charging field by which the particle was charged ( $\sim 3-5 \times 10^5$  V/m), and  $E_p$  is the precipitator electric field ( $\sim 3 \times 10^5$  V/m). The time it takes for a 1  $\mu\text{m}$  particle to drift in air to a collector that is 1 inch away is simply

$$t = \frac{d}{w} = \frac{\eta d}{\epsilon_0 a E_C E_p} = 0.57 \text{ seconds.}$$

Using this form of migration velocity the Deutsch equation can calculate the efficiency as a function of particle size as shown in Figure 3.

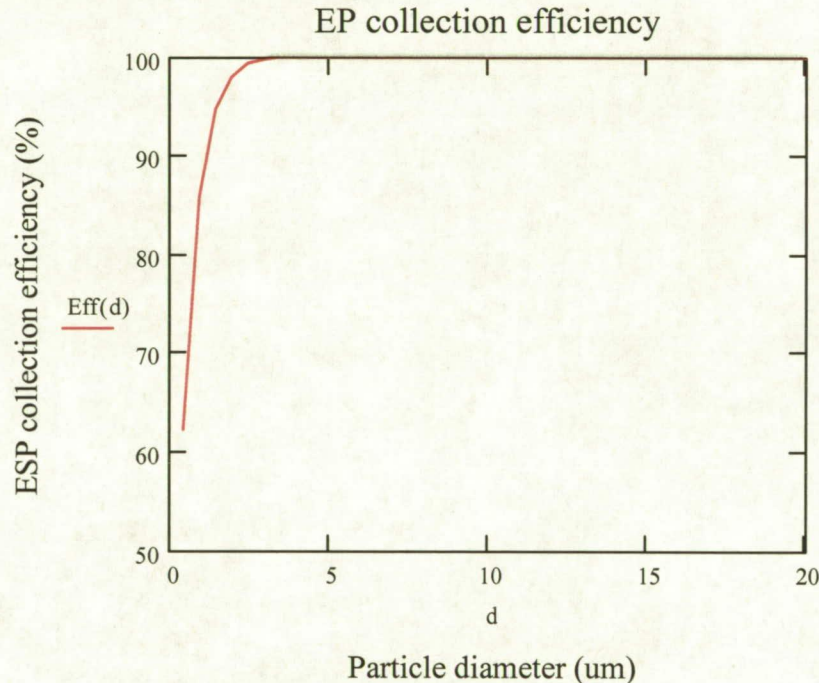


**Figure 3.** The EP efficiency as a function of particle size.

Note that the efficiency does not drop off until the particle size becomes extremely small since the migration velocity decreases for smaller particles.

One can also use the PSD to estimate precipitator efficiencies. For a log-normal distribution

$$\gamma(t) = \frac{1}{\sqrt{2\pi}} e^{-(t^2/2)}$$

White [4] has shown that modifications of the Deutsch equation have the form



$$Q = \frac{1}{\sqrt{2\pi}} \int_{-\infty}^{\infty} e^{-(t^2/2)} \cdot e^{-k\bar{x}e^{t \log \sigma}} dt$$

where  $\bar{x}$  is the geometric mean of the PSD,  $\sigma$  is the geometric standard deviation of the PSD and the parameter

$$k = 0.116 \frac{AE_c E_p}{\dot{V} \eta}$$

contains all of the information regarding the precipitator. MathCad was able to integrate the above equation using the black dust fitting parameters for  $\bar{x}$  and  $\sigma$  discussed earlier to give an overall efficiency of 0.988 or 98.8%.

### 3.0 Prototype EP

A 32 inch prototype electrostatic precipitator with a collection area of 0.13 m<sup>2</sup> made of 304 stainless steel was designed, built and tested. A high voltage stainless steel wire is suspended along the axis of the EP using a spring attached to a teardrop shaped ceramic insulator for electrical isolation. This end of the EP is made out of polycarbonate in order to allow the users to see inside the EP and check the resulting corona/glow discharge. The other end of the wire is attached to an MDC high voltage electrical vacuum feedthrough (part no. 642000) rated at 30 kV.

A schematic of the entire setup is shown in Figure 4. The EP is connected to GN<sub>2</sub> supplied by ALAC directly regulated at 220 lpm which corresponds to the highest demand that both the Kennedy Space Center and CCAFS system operates at during its maximum usage. Downstream of the regulator is a Top Trak model 822-S2-H-2 mass flow meter (not shown in Figure 4) with analogue signal output which monitors the incoming flow rate. Some of the dry GN<sub>2</sub> gas is diverted into the turn table housing box to acclimate the black dust supplied for testing. Delivering a continual stream of black dust to the EP utilized the Venturi effect method identical to that used by the TSI Model 3433 Small Scale Powder Dispenser to aerosolize dust. This was possible because of the large gas flow at the small inlet port expanded into a larger volume resulting in a net negative pressure even for a system at 20 psi. It is the negative pressure that allows suction through a small 1/16 inch capillary tube to deliver dust to the air flow at a rate of 2 lpm. The amount of dust that enters the tube is regulated by the speed at which the turntable rotates. The entire assembly is housed within the GN<sub>2</sub> gas to keep excess oxygen or air from entering the EP which would greatly alter the electrical breakdown properties of the gas. Any ozone or NO<sub>x</sub> gases resulting from electrical breakdown are vented outside the system.

In order not to interrupt the gas flow, dust concentrations were sampled isokinetically meaning there can be no pressure difference between the sampling tube and the surrounding gas. An isokinetic Pitot tube was used to sample the downstream gas flow directly into either a TSI DustTrak Aerosol Monitor or a Climet model Cl-150t portable Laser Particle Counter. The TSI DustTrak Aerosol Monitor is capable of monitoring dust concentrations as low as 0.001 mg/m<sup>3</sup>. [Room air has typical dust concentrations of ~0.008-0.010 mg/m<sup>3</sup>]. To match the required flow



rate of 1.7 l/m needed for the TSI DustTrak Aerosol Monitor for a gas flow velocity of 1.85 m/s, the isokinetic tube must have a radius of 0.088 inches or a diameter of 0.174 inches, which happens to be the inner diameter (ID) of standard ¼ inch tubing. The other method used to monitor dust concentration was a Climet model CL-150t portable Laser Particle Counter. This device counts particles in four particle size ranges: 0.3-0.5  $\mu\text{m}$ , 0.5-1.0  $\mu\text{m}$ , 1.0-5.0  $\mu\text{m}$ , and  $>5.0 \mu\text{m}$ .

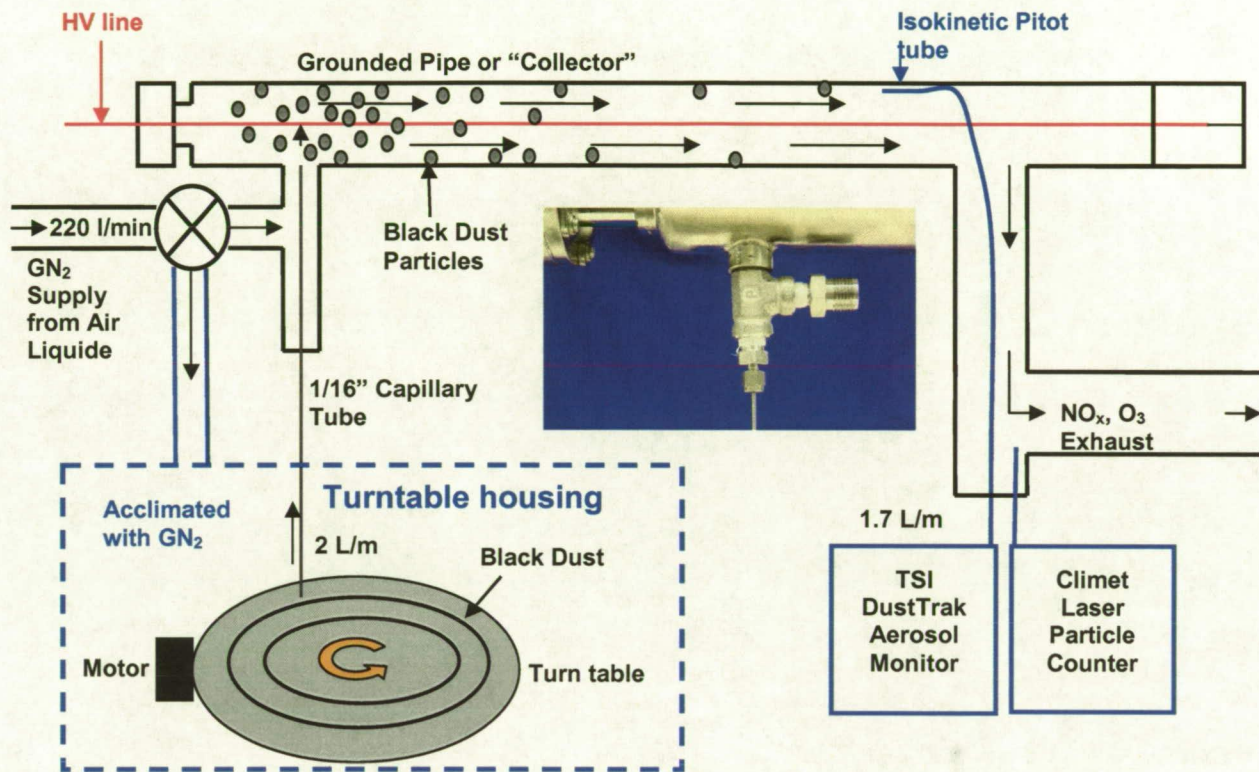


**Figure 4.** Air flow schematic of the EP demonstrating how the capillary tube is used to transfer the dust from the turn table to the EP. At the end of the EP an isokinetic Pitot tube samples the dust flow concentration measured by a TSI DustTrak Aerosol Monitor and a Climet model CL-150t Laser Particle Counter.

### 3.1 Current-Voltage Characteristics

Attempts to measure the current-voltage characteristics of the GN<sub>2</sub> were unsuccessful. Although impurity measurements of GN<sub>2</sub> line typically show that oxygen content can vary between 20 and 50 ppm, stable currents could not be realized with the minimal oxygen levels within the gas stream. Instead, as the application of high voltage (Spellman model RMP-300W) increased, an orange glow began to appear in the form of a star-shape followed by spark breakdown. This single point glow plagued all attempts to stabilize the current and the use of current limiting resistors were unsuccessful. Adding a 1 M $\Omega$  resistor did not increase the current as the voltage increased. After the voltage reached between -10 kV and -13 kV breakdown would occur. Adding a 100 M $\Omega$  resistor prevented breakdown (up to 30 kV) but did not allow current to flow.



A 5 M $\Omega$  resistor worked best to allow almost 5 mA of current to flow at low relatively voltages but the orange spot appeared. Other attempts to remove this breakdown were also unsuccessful. The electrostatic precipitator was cleaned thoroughly and the stainless steel wire replaced with an inconel wire. After the inconel wire tests were unsuccessful, new stainless steel wires were also replaced. Still the orange glow persisted and similar phenomenon has not been reported in the literature. However, it must be noted that the “step-like” form of the I-V curve was expected in nearly pure GN<sub>2</sub> in the absence of electronegative ions available for corona discharge.

### 3.2 Rotating Spark Gap System

The problems of using a DC voltage source may be overcome by using an AC signal. Many commercial systems use AC pulsed or fast-spark voltages due to the higher peak voltages available at the optimum spark rate, the inherent current-limiting action on spark surges, the higher electrical efficiencies, better overall stability, and higher collection efficiencies. Since the orange glow was unavoidable under application of high voltage DC signals, perhaps a short duration pulse superimposed over a high voltage DC signal would allow higher peak voltages and higher mean currents without sparkover and still increase particle charging. A background DC voltage is still a requirement since the charged particles must drift toward the collector, but the value need not be near the electrical breakdown voltage.

Researchers have shown that pulses with fast risetimes lead to a more uniform discharge at the high voltage electrode, eliminating local regions of high current density [5]. Efficiencies are attributed to a more uniform current distribution and the ability to regulate the current without reducing the peak voltage. It is generally believed that short pulses (5-500  $\mu$ s) spaced farther apart (50-100 ms) give the best improvement for efficiencies. Figure 5 shows a schematic of a new pulsed power supply capable of providing short pulses on top of a DC voltage in an effort to resolve the breakdown issues while improving the efficiency of the EP.

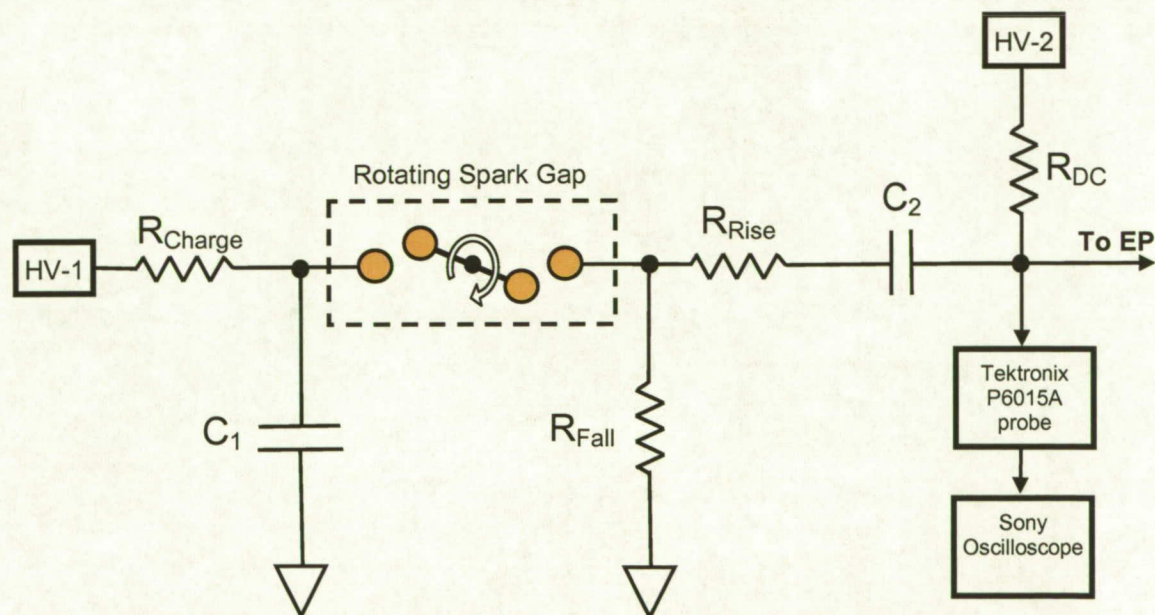


Figure 5. Wiring schematic of the pulsed power supply used for the EP.



The new power supply was developed in two phases. The first phase was needed to generate an HV pulsed AC signal to charge the particles, and the second phase was created to provide the DC background to attract the particles to the collection area. Each phase required its own separate power supplies to provide power to the EP. The first labeled HV-1 was a -60 kV Glassman EH Series High Voltage Power Supply which charges a high voltage RC circuit given by  $R_{\text{Charge}}C_1$  in Figure 5.  $R_{\text{Charge}}$  is a series of high voltage resistors rated at 20 Watts (each built by EGB) and is set to 2 M $\Omega$  while  $C_1$  is a series of high voltage capacitors rated up to 40 kV (each built by Murata) and has a value of 5 nF. Together they form an RC circuit with a decay time of 10 ms or 100 Hz (with 5 RC constants equal to 50 ms at a frequency of 20 Hz) that feeds a Rotating Spark Gap system.

Rotating Spark Gap systems are commonly used to create high voltage pulsed AC signal at frequencies greater than 10 Hz. The Rotating Spark Gap consists of two 0.75" diameter electrodes connected electrically with an aluminum rod spaced ~1 mm from two stationary electrodes held in place with Delrin® plastic. The rod is connected to a motor via an insulating Delrin® shaft and mounted with two ball bearings on both sides. The entire ensemble is housed in a polycarbonate box for safety considerations. The frequency of the pulse depends on the speed of rotation since sparks occur across both gaps once the electrodes are aligned horizontally. Thus the frequency of the sparks is easily controlled as long as the rotation speed is slower than the time it takes to charge up the RC circuit that charges the spark gap. Typical rotation speeds are 1719 RPM or 28.65 Hz.

The rise and fall time of the shape of the pulse is determined by  $R_{\text{Rise}}$  and  $R_{\text{Fall}}$ .  $R_{\text{Rise}}$  is set to 440  $\Omega$  which is as small as possible for a fast rise pulse while  $R_{\text{Fall}}$  is set a little higher to 5.6 k $\Omega$  to give a slightly longer fall time. The asymmetry of the spark may not be critical and after several iterations these values provided the best shape to ensure the highest voltages were reached consistently without affecting the other parameters. Since these resistors were going to absorb nearly all of the energy of the spark, they needed to be very high power liquid resistors that could not be purchased commercially. Thus they had to be fabricated in the laboratory using rubber hoses of certain dimensions filled with copper sulfate. Copper sulfate has a known conductivity at different concentrations so the resistance is calculated by knowing the length and radius of the resistor and the concentration of the copper sulfate. Figure 6 shows pictures of the rotating spark gap and the liquid resistors.

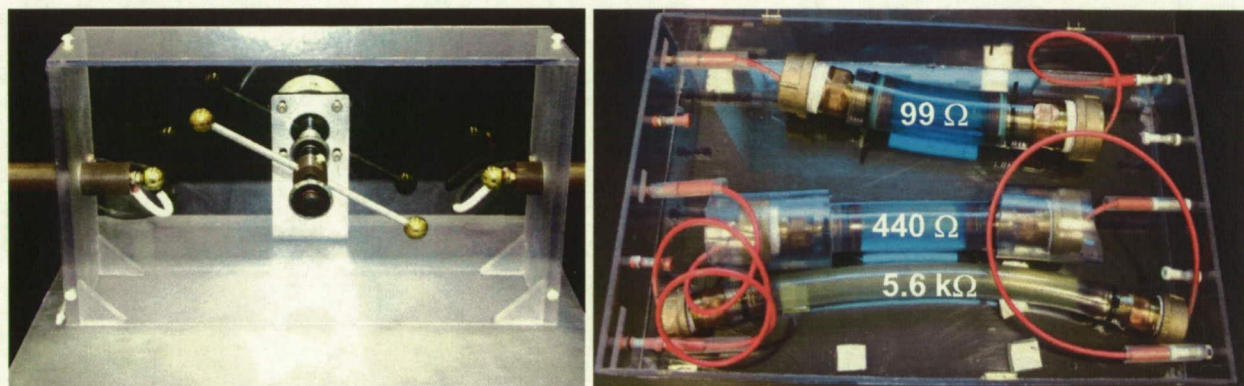


**Figure 6.** Pictures of the (left) Rotating Spark Gap and (right) liquid resistors used for the pulsed power supply.



The second phase of the design consisted of the DC offset required to create an electric field strong enough to move the charged particles to the collection area (sides of the pipe). A Glassman EH Series High Voltage Power Supply provided the DC signal which was kept just below the breakdown limit of -10 kV to prevent the orange glow. At this voltage the electric field would be strong enough to move charged black dust particles but not produce any form of electrical breakdown.. The power supply was protected using a 20 Watt-rated high power resistor set to 30 M $\Omega$  which limited the current out of the Glassman and served to protect it from the pulsed waveforms generated in the Rotating Spark Gap.

Finally the two phases were connected together and attached to the EP. A 2200 pF high voltage Murata capacitor labeled C<sub>2</sub> was used to isolate the DC phase from the pulsed AC phase. The waveform going into the EP was monitored using a Sony Tektronix P6015A High Voltage Probe with an internal resistance of 100 M $\Omega$  connected to an oscilloscope.

Typical waveform pulses delivered to the EP are shown in Figure 7. There are approximately 17-19 pulses per second, which is consistent with a rotation spark gap frequency  $\sim 30$  Hz (there are two pulses per revolution one for each half turn). Many of the pulse peaks cannot be seen on the 0.2 ms scale of the graph. Typical rise times for  $R_{\text{Rise}} = 440 \Omega$  and fall times for  $R_{\text{Fall}} = 5.6 \text{ k}$  are on the order of 50  $\mu\text{s}$  which may be too small to be seen on this scale. There are however, some pulses which lasted a little longer can be seen to have reached values of about -9.2 kV in Figure 7. The output of the high voltage power supply HV-1 measured a peak voltage of about -15 kV for each spark. The peak voltage height can be adjusted by simply changing the separation distance between the fixed and rotating spark gap electrodes.

One phenomenon which remains not fully understood is why the potential tries to approach zero after each pulse even though there is an applied -10 kV DC offset. Early tests in many cases showed the potential going above zero which eliminates the DC field necessary to direct the particles toward the ground. Changing the  $R_{\text{DC}}$  values remedied this situation. With an internal resistance of 100 M $\Omega$  one can see the effect that the Sony Tektronix probe had on the system. It acts as a voltage divider to lower the -10 kV output of HV-2 when connected up in parallel with the EP according to Figure 5 by

$$V_M = \frac{-10}{\left(\frac{R_{\text{DC}}}{100} + 1\right)}$$

where  $V_M$  is measured in kV and  $R_{\text{DC}}$  in M $\Omega$ . As  $R_{\text{DC}}$  gets larger, the DC voltage on the HV wire of the EP gets smaller. Experimentally reducing  $R_{\text{DC}}$  from 50 M $\Omega$  to 30 M $\Omega$  ensured that the potential was negative inside the precipitator at all times to provide a net negative electric field necessary to allow the charged dust particles to drift toward the grounded pipe. In Figure 7 the overall average potential was -3.73 kV.

After the spark, the lowered potential rises toward its DC background value of  $V_M = -7.69 \text{ kV}$  (for  $R_{\text{DC}} = 30 \text{ M}\Omega$ ) but does not reach it before the subsequent spark. The lowered potential could be a result of the increased space charge around the HV wire created by the spark since each one represents a small electrical breakdown of the gas. The spark causes the wire to emit a



cloud of electrons that attach to the much heavier nitrogen molecules that move toward the grounded pipe. At the time of breakdown, the potential difference between the high voltage wire and the nearby electron cloud may be close to zero (both consisting of negative electron charges) and begins to increase as the charged dust cloud approaches the ground plan. This may account for the sudden drop in potential that quickly recovers between sparks.

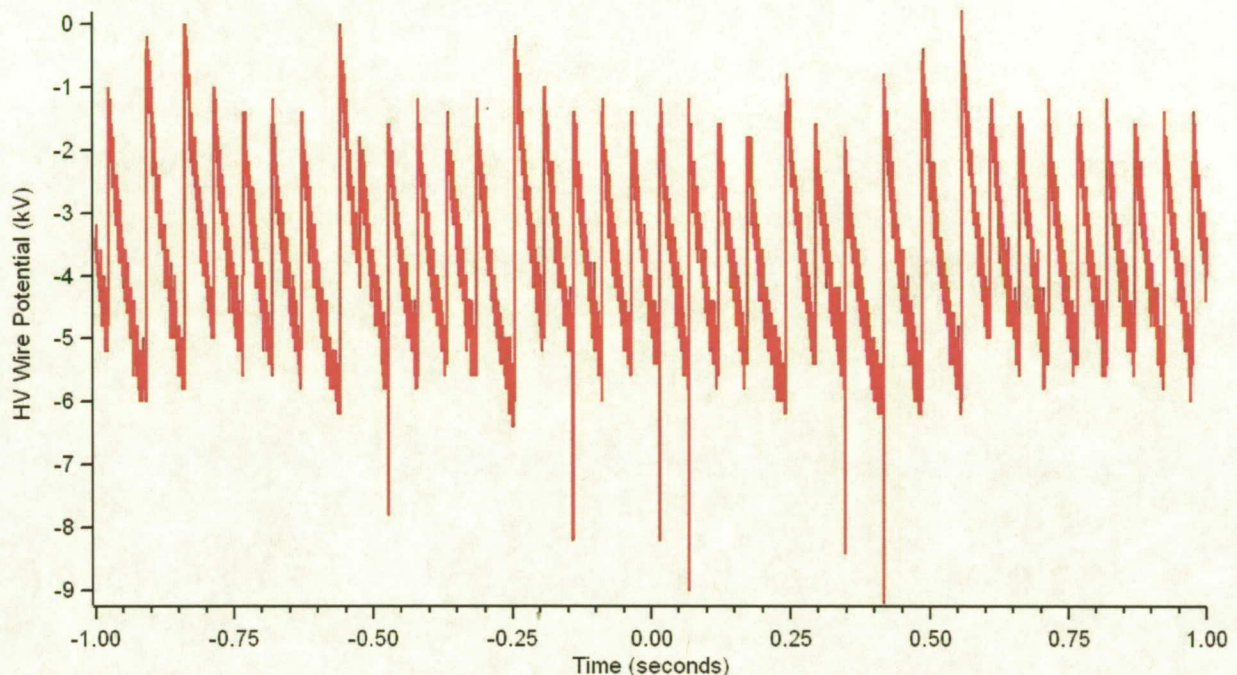


**Figure 7.** Sample waveform delivered to the EP from both the Rotating Spark Gap and application of a HV DC offset.

Finally, the application of this voltage waveform did not cause major current leakage or other breakdown problem which might limit the voltage applied. Corona was detected in the form of an even purple glow along the length of the wire without any signs of the orange-like discharge. The only issue that was of concern was whether the DC voltage was high enough to trap charged black dust particles.



## 4.0 Experimental Results

Testing of the collection efficiencies using the new pulsed-power supply were performed using actual GN<sub>2</sub> supplied directly from Air Liquide. There were several tests ran using the EP under various conditions which showed the usefulness of the technique. The first condition consisted of testing the gaseous nitrogen “as delivered” without the addition of more black dust. The Climet 150t Laser Particle Counter is ideal for clean gas monitoring of a relatively small number of dust particles per unit time. The device operates in one minute increments during each sample. The average values for 10 samples of room air, GN<sub>2</sub> with the precipitator off and GN<sub>2</sub> with the precipitator on, are presented in Table 1. Clearly the room air was far more contaminated than the gas delivered from Air Liquide. This is not surprising, considering the great lengths that go into filtering the GN<sub>2</sub> for each customer. Still, it is too contaminated for many customers that require stringent cleanliness, since particles are easily able to transport through the current filter elements.

A great reduction of particle counts can be realized when using an electrostatic precipitator as seen by the efficiencies measured for each particle size range in Table 1. It is important to note that these results show that a 74%-87% reduction can be seen by simply turning on the EP without thoroughly cleaning the piping and housing of the Climet between tests. These preliminary results are very encouraging since they were obtained in its current configuration before optimization.

**Table 1.** Number of particles detected using the Climet Laser Particle Counter.

	Particle Size Range (µm)			
	0.3-0.5	0.5-1.0	1.0-5.0	> 5.0 µm
<b>Room Air</b>	41,900,936	4,607,769	772,218	10,863
<b>EP OFF with GN<sub>2</sub></b>	4,498,389	1,297,001	85,419	696
<b>EP ON with GN<sub>2</sub></b>	985,459	162,136	11,597	180
<b>EP Efficiency</b>	78.09	87.50	86.42	74.20

The TSI DustTrak Aerosol Monitor also showed a significant decrease in the concentration of particles in the as-delivered GN<sub>2</sub>. Figure 8 shows the results of the gas with the EP off and the subsequent concentration reduction with the EP on. These measurements were taken after cleaning the precipitator to ensure that particles came from the gas as delivered. An average concentration of about 11.4 µg/m<sup>3</sup> per second is given as the background from the gas lines of Air Liquide. Once the precipitator is on, this concentration reduces to 8.56 µg/m<sup>3</sup> which is a 25% reduction in concentration. However, this lower measured concentration approached the resolution limit of the device, which is capable of only measuring down to ~8 µg/m<sup>3</sup> so the actual amount of material removed cannot be measured with the TSI DustTrak. It is very likely that the final real concentration is much lower, as indicated by the Climet results above.



The next step was to add black dust to the flow in order to measure the collection efficiencies with greater accuracy. The setup to deliver this dust was described earlier. The black dust used was actual material removed from filter elements within the lines themselves.

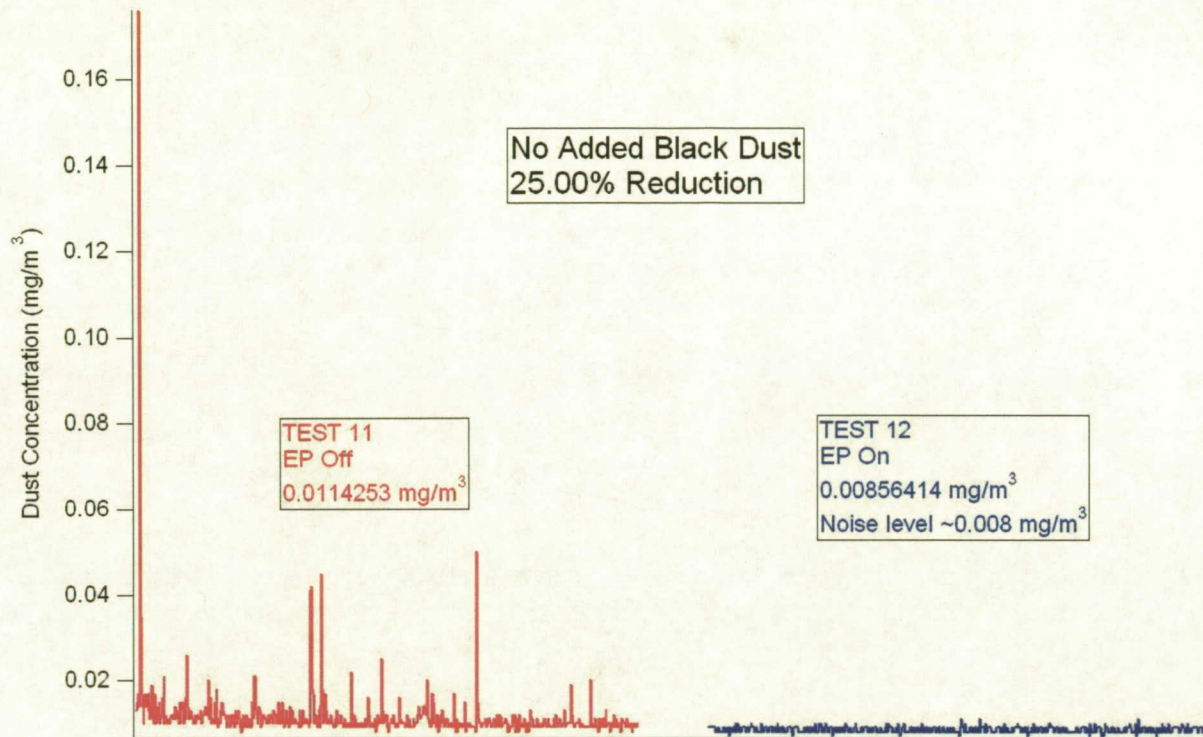


**Figure 8.** The TSI DustTrak measured concentrations of as-delivered  $\text{GN}_2$  with the precipitator off (red) and the precipitator on (blue). Each measurement was performed over a 10 minute period.

Several tests were ran using additional black dust. The turntable supplied an average dust loading per second of about  $107 \text{ mg/m}^3$ , which is almost 10,000 times that of the background as-delivered  $\text{GN}_2$  lines. At this extreme concentration, any method to remove this amount of dust loading could be considered a successful test under worst-case conditions. Adding additional dust not only allows for accurate measurements of the precipitator's efficiency which Figure 8 cannot supply, but also provided an accurate account of how the efficiency would degrade in time. The additional dust simulates an accelerated particle deposition on the collector surface which degrades efficiency over time. With this information, it would be possible to predict when the efficiency drops below an unacceptable level of 90%, which indicates to the user that cleaning is required.

One early goal was to increase the overall DC potential by changing  $R_{\text{DC}}$ . Once the correct choice of resistance was found, efficiencies above 99% were commonplace. A typical data set is shown in Figure 9. The large peaks in the data indicate the dust measured with the EP turned off while the reduced values in between the peaks signify when the EP is turned on. Average concentrations of each set are shown in the textboxes. Individual collector efficiencies are calculated by difference in concentrations with between the EP on and off divided by the concentration of the EP off or  $[(\text{EP}_{\text{Off}} - \text{EP}_{\text{On}})/\text{EP}_{\text{Off}}] \times 100\%$ . Figure 9 shows the overall average



dust loading supplied by the turntable was  $106.83 \text{ mg/m}^3$  which was reduced to  $0.510 \text{ mg/m}^3$  with the EP on. This corresponds to an average efficiency of 99.52%

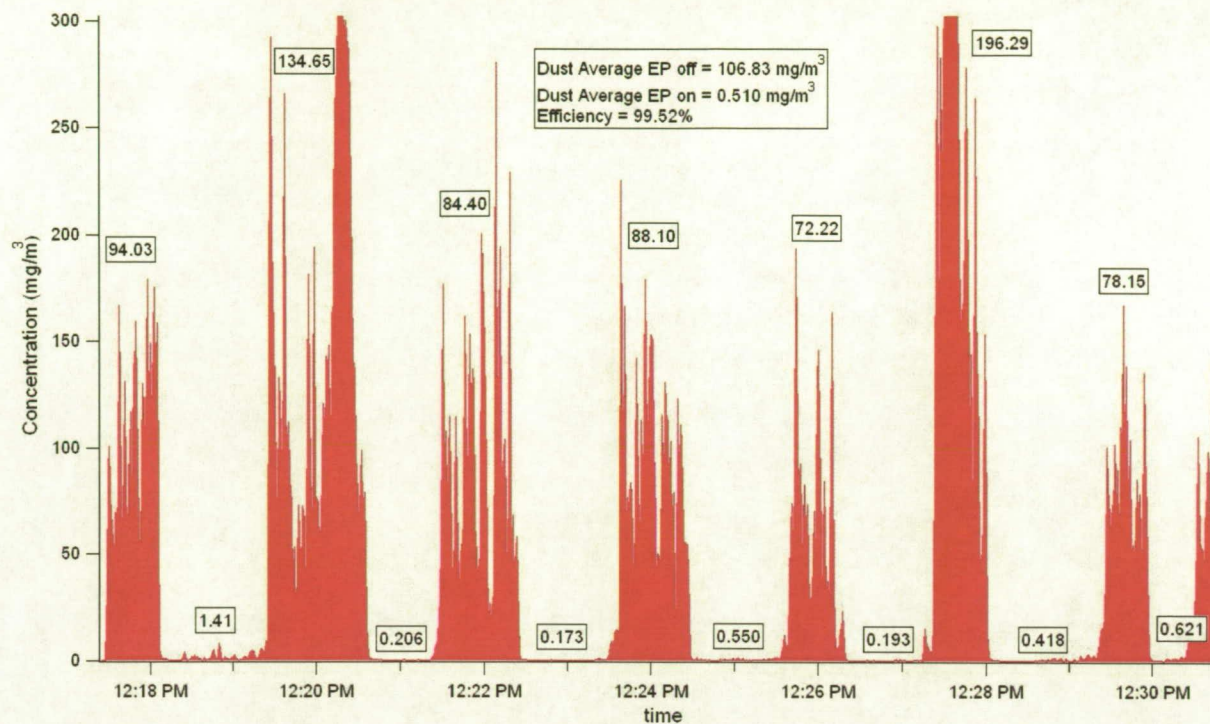


Figure 9. A sample data set of the measured black dust concentrations turning the precipitator on and off.

These results show greater than 99% efficiencies using this rotating spark gap power system. The long purple glow along the length of the HV wire signified the presence of the corona which successfully charged the particles. Only a small net DC electric field was required to move and trap the charged black dust to the walls to be collected. Upon closer inspection of Figure 9 one can see that the amount of dust input to the EP exceeded the measurement capabilities of the DustTrak which meant that the real efficiencies in some cases were actually higher than presented.

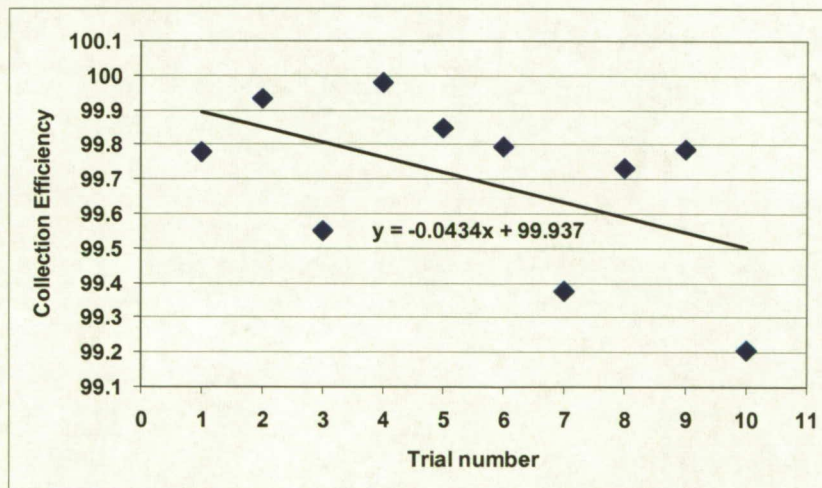


Figure 10. The change in collection efficiency over time.



Cleaning efficiencies degraded in time, which is not surprising considering the excess dust loading into the precipitator. Figure 10 highlights the slight decrease in efficiency which decreases about 0.0434% with each trial that lasts one minute in duration. The total amount deposited onto the collector surface per unit area  $DEP(t)$  is given by

$$DEP(t) = A_{IN} \int Eff(t) dt$$

where  $A_{IN}$  is the incoming dust concentration, which is not expected to be a function of time, times the integral of the efficiency given as

$$Eff(t) = -0.000434t + 0.99937.$$

Assuming that the precipitator needs to be cleaned when the efficiency reaches 90% amounts to a cumulative dust loading of  $23,270 \text{ mg/m}^3$  for our current dust-loaded system corresponding to about 229 laboratory tests ( $\sim 8$  hours of testing). Noting that the current  $\text{GN}_2$  system only deposits  $0.0114253 \text{ mg/m}^3$  per second would take  $2.0367 \times 10^6$  seconds or 23.5 days to acquire the same dust loading. Thus the EP would only have to be cleaned about once per month to ensure greater than 90% efficiencies. Commercial precipitators typically consist of flat parallel plates that are usually rapped every few minutes. Such frequent cleanings would ensure efficiencies greater than 99% at all times for an EP built for this system.

## 5.0 Conclusions

Electrostatic precipitation has been shown to be a viable alternative to conventional filtration methods for removing black dust contaminants even in nearly pure gaseous nitrogen environments. The rotating spark gap system devised to supply the corona in parallel with a high voltage DC offset was successful in charging and trapping fine black dust particles. A system of this sort could be used to remove contaminants from the  $\text{GN}_2$  lines here at KSC and CCAFS.

## Acknowledgements

The authors wish to thank NASA's CTC program for funding this project as well as Chuck Davis (NASA TA-E3) for continual support.



## References

1. Gibson, T., et al., *Black Powder (Dust) Phenomena Study*. 2005, ASRC Aerospace: Kennedy Space Center, FL.
2. ASTM, *Standard Test Method for AC Loss Characteristics and Permittivity (Dielectric Constant) of Solid Electrical Insulation*. ASTM D 150 - 98 2004.
3. Kolmogorov, A.N., *Über das logarithmisch normale verteilungs gesetz dr Teilchen bei zerstückelung*. Comptes Rendus (Dioklady) de l'Academie des Sciences de l'U.S.S.R., 1941. 31.
4. White, H.J., *Industrial Electrostatic Precipitation*. 1963, Reading, MA: Addison-Wesley.
5. Cross, J., *Electrostatics: Principles, Problems and Applications*. 1987, Bristol, England: IOP Publishing Limited Techno House.
6. Buhler, C.R., et al., *Electrostatic Precipitation of Black Dust from GN2*. CTC 2006 Phase I Final Report 2006.